Chapter 3

Quantitative proteomics reveals extensive changes in the ubiquitinome after perturbation of the proteasome by targeted dsRNA mediated subunit knockdown in *Drosophila*.

Karen A. Sap, Karel Bezstarosti, Dick H. W. Dekkers, Olaf Voets,

Jeroen A. A. Demmers

Published in Journal of Proteome Research (2017)

Abstract

The ubiquitin–proteasome system (UPS), a highly regulated mechanism including the active marking of proteins by ubiquitin in order to be degraded, is critical in regulating proteostasis. Dysfunctioning of the UPS has been implicated in diseases such as cancer and neurodegenerative disorders. Here, we investigate the effects of proteasome malfunctioning on global proteome and ubiquitinome dynamics using SILAC proteomics in *Drosophila* S2 cells. dsRNA mediated knockdown of specific proteasome target subunits is used to inactivate the proteasome. Upon this perturbation, both the global proteome and the ubiquitinome become modified to a great extent, the overall impact on the ubiquitinome being most dramatic. The abundances of approx. 10% of all proteins are increased, while the abundances of the far majority of over 14 thousand detected diGly peptides are increased, suggesting that the pool of ubiquitinated proteins is highly dynamic. Remarkably, several proteins show heterogeneous ubiquitination dynamics, with different lysine residues on the same protein showing either increased or decreased ubiquitination. This suggests the occurrence of simultaneous and functionally different ubiquitination events. This strategy offers a powerful tool to study the response of the ubiquitinome upon interruption of normal UPS activity by targeted interference and opens up new avenues for the dissection of the mode of action of individual components of the proteasome. Since this is to our knowledge the first comprehensive ubiquitinome screen upon proteasome malfunctioning in a fruit fly cell system, this data set will serve as a valuable repository for the *Drosophila* community.

Introduction

In eukaryotic cells, short-lived, regulatory, misfolded and denatured proteins are degraded by the ubiquitin–proteasome system (UPS), a highly regulated mechanism involving the active marking of proteins for proteasomal degradation by ubiquitin. The 26S proteasome is the central protease in nonlysosomal ubiquitin-dependent degradation. It is involved in diverse processes such as protein quality control, antigen processing, signal transduction, cell cycle control, cell differentiation and apoptosis (Hershko and Ciechanover, 1998) and, as such, is critical in regulating proteostasis. Aberrations in the UPS have been implicated in cancers and in the pathogenesis of neurodegenerative diseases, such as Parkinson's (PD), Alzheimer's (AD), Huntington's (HD), prion diseases, as well as amyotrophic lateral sclerosis (ALS) (Keller, Gee and Ding, 2002; Ciechanover and Brundin, 2003; Giasson and Lee, 2003). The critical roles played by ubiquitin-mediated protein turnover in cell cycle regulation makes this process a target for oncogenic mutations. The proteasome serves as a target for cancer chemotherapy, as exemplified by bortezomib (Velcade), a proteasome inhibitor that binds proteolytic pockets in

the 20S core (Groll *et al.*, 2006; San Miguel *et al.*, 2008). Proteasome inhibitors exert anti-tumor activity *in vivo* and potently induce apoptosis in tumor cells *in vitro* (Almond and Cohen, 2002).

Ubiquitylation, the covalent attachment of ubiquitin to the ε-amino group of substrate lysine (Lys) residues, is a versatile posttranslational modification (PTM). A key feature of ubiquitin is its ability to form polymeric chains, in which individual moieties are linked via one of seven Lys residues or the N-terminal methionine (Komander, 2009). Only a few of these distinct linkage types have been studied extensively: K48-linked polyubiquitin serves as a targeting signal for proteasomal degradation (Chau *et al.*, 1989), whereas K63-linked polyubiquitin is thought to be involved in cell signaling, membrane trafficking, and the DNA damage response (Chen and Sun, 2009). K11-linked polyubiquitin has been suggested to have both degradative and non-degradative roles (Xu *et al.*, 2009), while the M1-linkage has a crucial role in the canonical NF-κB activation pathway (Iwai and Tokunaga, 2009). The biological significance of ubiquitin chains linked through K6, K27, K29, or K33 is still poorly understood (Komander and Rape, 2012).

Over the past years, proteomic tools have been developed to identify and quantify ubiquitin-dependent signaling systems and to elucidate details of UPS functioning (Kim, Eric J. Bennett, *et al.*, 2011; Wagner *et al.*, 2011; Udeshi *et al.*, 2013; Ordureau, M??nch and Harper, 2015). These novel technologies to study global protein ubiquitination (the 'ubiquitinome') are based on highly specific antibody enrichment of peptides carrying the diGly remnant motif as a result of tryptic cleavage of ubiquitinated proteins and have taken over low- to medium-throughput approaches (*e.g.*, (Mayor *et al.*, 2007)). The diGly peptide enrichment technology has been applied *e.g.* to study ubiquitylation site specificity and topology of PARKIN-dependent target modification in response to mitochondrial depolarization (Sarraf *et al.*, 2013), to find novel substrates of HUWE1 using an inducible loss of function approach (Thompson *et al.*, 2014), and, recently, to identify specific substrates of a novel class of proteasome inhibitors (capzimin) (Li *et al.*, 2017).

Here, we investigate the effect of proteasome inhibition on the global cellular proteome and the ubiquitinome-by means of SILAC based proteomics. Two different approaches to inactivate the proteasome are compared: first, by the addition of the chemical agents MG132 (Lee and Goldberg, 1998a) and Lactacystin (Fenteany *et al.*, 1995), which target the proteolytic activity of the proteasome; second, by double-stranded RNA (dsRNA)-mediated interference (RNAi) of proteasome subunit gene expression. The latter approach presents several advantages in investigating the molecular mechanisms of the UPS, since individual functional subunits can be inactivated by RNAi in a highly selective manner in *Drosophila* cells, as has been shown before by various groups (Wójcik and DeMartino, 2002; Lundgren *et al.*, 2003; Elena Koulich, Xiaohua Li, 2008). *Drosophila* cell systems in general provide an excellent tool to study basic cellular processes and subsequent translation to the whole organism is relatively straightforward. The fruit fly has an established role as a model system for the study of the nervous system in general and the role of proteasome impairment and neurodegeneration in particular (Yeh, Jansen and

Schmidt-Glenewinkel, 2011). There is a public collection of transgenic flies available, accommodating over 22,000 different transgenic fly lines that provide knockdowns for over 88 % of *Drosophila* genes (Dietzl *et al.*, 2007). Expression of these transgenic RNAi constructs can even be driven in a tissue specific manner (Brand and Perrimon, 1993), providing a simple yet powerful strategy to study the role of individual genes in diverse biological processes.

Our results reveal that a substantial part of the detectable global proteome is affected in cells that have (partially) inactivated proteasomes. The ubiquitinome analysis based on > 14,000 identified diGly peptides (of which > 11,000 could be quantified), revealed that the far majority of all ubiquitination sites are upregulated after inactivation of the proteasome, indicating that the pool of ubiquitinated proteins and the extent of ubiquitination are highly dynamic. We highlight several interesting examples of proteins with different target Lys residues showing either increased or decreased ubiquitination, which suggests the occurrence of simultaneous and functionally different ubiquitination events on a single protein or protein population.

In conclusion, we show that manipulation of proteasome functioning by targeted dsRNA mediated perturbation in *Drosophila* has major effects on the global cellular proteome and ubiquitinome. The novelty of this work lies in 1) the combination of ubiquitinome profiling with dsRNA mediated knockdown of proteasome subunits, 2) mimicking complete proteasome inactivation by dsRNA mediated knockdown of a dedicated selection of multiple subunits, and, 3) the use of *Drosophila* as the model organism for ubiquitinome profiling. The strategy applied here opens up avenues for the dissection of the mode of action of this intriguing cellular machinery by knocking down every single protein building block, both under proteostasis as well as abnormal conditions. As this study is the first large-scale investigation of protein ubiquitination in a *Drosophila* model system, it provides a valuable source of information for the community at large.

Material and Methods

Cell culture and sample preparation: *Drosophila melanogaster* Schneider's line 2 cells (S2 cells, R690-07, Invitrogen) were cultured in Schneider's medium (Invitrogen) supplemented with 10% fetal calf serum (Thermo) and 1% penicillin-streptomycin.

Antigen production: Full length cDNA of RPN11, Prosalpha5, Prosbeta6, RPN8, RPN10, RPT4 and C-terminal (aa 220–405) RPT6, were cloned into pGEX-2TKN vectors (Pharmacia). GST fusion protein expression, purification, and subsequent immunization were performed as described previously (Chalkley and Verrijzer, 2004). Other antibodies used were α-FK2 and α-polyubiquitin SPA-200 (both Enzo Life Sciences), 20S- α (sc- 65755) (Santa Cruz Biotechnology), and α-H2B (described in (Chalkley and Verrijzer, 2004)), dGMPS (described in

(Reddy *et al.*, 2014)) and dISWI (described in (Kal *et al.*, 2000)). Immunoblotting assays were performed using standard procedures.

FACS analysis: FACS analysis was performed essentially as described in (Moshkin *et al.*, 2007).

Glycerol gradients: Glycerol gradients were prepared essentially as described previously (Mohrmann *et al.*, 2004). Briefly, 5-30% gradients were generated in Beckman polyallomer tubes (331374). Whole cell lysates were prepared under non-denaturating conditions in 50 mM HEPES-KOH pH 7.6 / 100 mM KCl / 0.1% NP40, including protease inhibitors and loaded on top of the gradient and ultracentrifuged at 32 krpm for 17 h at 4°C (Beckman L-80 SW40 rotor). Thirteen 500 µl fractions were taken starting from the top of the gradient and fractions were analyzed by immunoblotting.

SILAC labeling: S2 cells were grown in custom made Schneider's medium (Athena Enzyme Systems, Baltimore, MD). This medium is based on Schneider's *Drosophila* medium from Invitrogen (#21720024) but is deficient for both lysine and arginine and contains dialyzed yeastolate (3,500 kDa MWCO). Before use, the medium is supplemented with 10% dialyzed fetal bovine serum (F0392, Sigma-Aldrich), 1% penicillin-streptomycin and 2 mg/ml light ($^{12}C_6$) lysine (A6969, Sigma-Aldrich) and 0.5 mg/ml light ($^{12}C_6$, $^{14}N_4$) arginine (L5751, Sigma-Aldrich), or heavy ($^{13}C_6$) lysine (CLM-2247, Cambridge Isotope laboratories) and heavy ($^{13}C_6$, $^{15}N_4$) arginine (CNLM-539, Cambridge Isotope Laboratories). Cells were cultured at 27°C for at least 7 cell doublings to reach complete labelling. Duplicate experiments were carried out by 'label swapping', *i.e.* switching the isotopically labeled state of the control *c.q.* treated cells and *vice versa* (termed 'forward' and 'reverse' here).

Proteasome inhibition: Cells were treated with 50 µM MG132 (Calbiochem) and 5 µM Lactacystin (Cayman Chemical) simultaneously, both dissolved in a 2000x DMSO stock solution. Mock samples were treated with equal volumes of DMSO. Cells were incubated for 4h or 16h at 27 °C.

dsRNA constructs: Constructs were synthesized using the Ambion Megascript T7 kit according to the manufacturer's protocol. Knockdown experiments were further performed as described previously (Worby, Simonson-Leff and Dixon, 2001). For dsRNA mediated targeted proteasome subunit knockdown, S2 cells were treated with dsRNA constructs directed against Prosalpha5 (Uniprot identifier Q95083), Prosbeta6 (P40304) and RPN11 (Q9V3H2). Mock samples were treated with dsRNA directed against GFP, which is absent in the cell lines used for these experiments. The final concentration of total dsRNA was 6 µg/ml. S2 cells were incubated with dsRNA for either 48h or 96h at 27°C.

SILAC sample preparation: Cells grown in SILAC light or heavy medium were harvested and used for immunoblotting or proteome and ubiquitinome analyses. For immunoblotting, cells

were washed three times with ice-cold PBS and spun down for 5 min at 1,100 rpm at 4°C. Cell pellets were lysed in SDS-PAGE sample buffer and sonicated as described earlier. BCA assays (Pierce) were used to estimate protein concentrations. After proteasome perturbation with either inhibitors or dsRNA mediated knockdown, cells were mixed in a 1:1 ratio based on cell count. Cells were washed three times with ice-cold PBS and lysed in 200 µl of an 8 M urea / 50 mM Tris-HCl pH 8.0 / 50 mM NaCl lysis buffer (7 ml of this buffer was used for lysates for diGly enrichment IP assays). Lysates were then incubated on ice for 10 min, sonicated, and debris was removed by centrifugation. BCA assays were used to estimate protein concentrations. 20 mg total protein was used for diGly peptide enrichment for ubiquitinome analyses; for global proteome analyses 0.5 mg lysate was used. All SILAC experiments were performed in duplicate, *i.e.* in a 'forward' and 'reverse' manner.

Cycloheximide treatment: Cells were treated with either 50 µM cycloheximide (CHX, Sigma), with 50 µM cycloheximide plus MG132/Lactacystin or with with MG132/Lactacystin alone, or mock treated with DMSO. Cell cultures were treated with CHX 1 h before MG132/Lactacystin was added for 4 h. Treated and control cell cultures were then mixed in a 1:1 ratio based on cell count and prepared for further analysis.

Protein digestion and fractionation: Protein lysates were reduced with 10 mM dithiotreitol (DTT) for 1 h at room temperature followed by alkylation with 55 mM chloroacetamide (CAM) for 1 h in the dark. The mixture was diluted four times with 50 mM ammonium bicarbonate buffer before the addition of $CaCl_2$ (1 mM final concentration). Proteins were digested with sequencing grade trypsin (1:100 (w:w), Roche) overnight at room temperature. Alternatively, proteins were digested with LysC (1:100 (w:w), Wako Chemicals) for 1 h at room temperature before trypsinization. Protein digests were desalted using a Sep-Pak tC18 Vac cartridge (Waters) and eluted with 80% acetonitrile (AcN). Tryptic peptides were fractionated by HILIC on an Agilent 1100 HPLC system using a 5 µm particle size 4.6 x 250 mm TSKgel amide-80 column (Tosoh Biosciences). 200 µg of tryptic digest in 80% AcN was loaded onto the column. Peptides were eluted using a non-linear gradient from 80% B (100% AcN) to 100% A (20 mM ammonium formate in water) with a flow of 1 ml/min. Sixteen 6 ml fractions were collected, lyophilized and pooled into 8 final fractions. Each fraction was then analyzed by nanoflow LC-MS/MS as described below.

DiGly peptide enrichment: DiGly-modified peptides were enriched by immunoprecipitation using PTMScan® ubiquitin remnant motif (K-ε-GG) antibody bead conjugate (Cell Signaling Technology) starting from 20 mg total protein, essentially according to the manufacturer's protocol. Unbound peptides were removed by washing and the captured peptides were eluted with a low pH buffer. Eluted peptides were analyzed by nanoflow LC-MS/MS as described below.

Nanoflow LC-MS/MS: was performed on an EASY-nLC system (Thermo) coupled to a Q Exactive mass spectrometer (Thermo), operating in positive mode and equipped with a nanospray source. Peptide mixtures were trapped on a ReproSil C18 reversed phase column (Dr Maisch GmbH; column dimensions 1.5 cm × 100 μm, packed in-house) at a flow rate of 8 μl/min. Peptide separation was performed on ReproSil C18 reversed phase column (Dr Maisch GmbH; column dimensions 15 cm × 50 μm, packed in-house) using a linear gradient from 0 to 80% B (A = 0.1% FA; B = 80% (v/v) AcN, 0.1 % FA) in 70 or 120 min and at a constant flow rate of 250 nl/min. The column eluent was directly sprayed into the ESI source of the mass spectrometer. All mass spectra were acquired in profile mode. The resolution in MS1 mode was set to 70,000 (AGC: 3E6), the m/z range 350-1700. Fragmentation of precursors was performed in data-dependent mode by HCD (Top15) with a precursor window of 3.0 m/z and a normalized collision energy between 26.0 and 28.0. MS2 spectra were recorded with a resolution of 17,500 (AGC: 5E4). Singly charged precursors were excluded from fragmentation. Dynamic exclusion was set to 20 seconds and the intensity threshold was set to 8E3. For the ubiquitinome analysis, a single LC-MS/MS run was performed for all immunoprecipitated peptide material from one sample.

Data analysis: Mass spectrometric raw data were analyzed using the MaxQuant software suite (version 1.5.2.8 (Tyanova, Temu and Cox, 2016)) for identification and relative quantification of proteins. A false discovery rate (FDR) of 0.01 for proteins and peptides and a minimum peptide length of 6 amino acids were required. The Andromeda search engine was used to search the MS/MS spectra against the *Drosophila melanogaster* Uniprot database (release DROME_2014_10.fasta, containing 23,336 entries) concatenated with the reversed versions of all sequences and a contaminant database listing typical background proteins and supplemented with several known *Drosophila* viral proteins. A maximum of two missed cleavages were allowed. Q Exactive spectra were analyzed using MaxQuant's default settings for Orbitrap spectra, including a main search peptide and MS/MS match tolerance of 4.5 and 20 ppm, respectively. The maximum precursor ion charge state used for searching was 7 and the enzyme specificity was set to trypsin. Further modifications were cysteine carbamidomethylation (fixed) as well as protein methionine oxidation, Lys ubiquitination and STY phosphorylation (variable). The minimum number of razor and unique peptides was set to 1. Heavy-to-light (H:L) ratios were calculated using MaxQuant's default settings, including a minimum ratio count of 2 for label based protein quantification and of 1 for diGly peptide quantification. Only unique and razor non-modified, methionine oxidized and protein N-terminal acetylated peptides were used for protein quantitation. The 'requantify' option was selected in all cases. The minimum score for modified peptides was set to 40 (default value). Only proteins that were identified and quantified both in the forward and reverse assays and with consistent ratios were taken into account for further analysis. Protein sets were further analyzed with Perseus (Tyanova *et al.*, 2016) (version 1.5.0.15), the gene ontology (GO) software DAVID (version 6.7, available from

http://david.abcc.ncifcrf.gov/, (Huang *et al.*, 2007)) and in-house developed software (Sap *et al.*, 2015). For the statistical testing of quantitative data, we used either two-sided two-sample t-test were performed in Perseus using 250 randomizations and settings FDR=0.05 and S0=0.5 or 'significance B' with p-value=0.05. For these statistical tests, additional control experiments were considered in which light and heavy labeled non-treated cells were mixed in a forward and reverse fashion. Hierarchical clustering was performed using the following settings: row tree: distance Euclidian; linkage: average; number of clusters: 300; column tree: distance Euclidian; linkage: average; number of clusters: 300.

MS raw data and data for protein identification and quantification were submitted as supplementary tables to the ProteomeXchange Consortium via the PRIDE partner repository with the data identifier PXD002552.

Results and Discussion

In order to investigate proteasome dysfunction by either chemical drugs or dsRNA mediated knockdown of specific subunits, we took a quantitative proteomics approach in *Drosophila*. We set off by selecting a combination of catalytic, structural and regulatory subunits that, when simultaneously depleted, resulted in abolishment of all proteasomal activity. Single dsRNA mediated knockdown for several subunits was performed but did not result in sufficient knockdown in all cases (results not shown). The most efficient knockdowns for individual subunits were obtained with Prosalpha5, Prosbeta6 and RPN11 (Figure S1A). Protein levels after four days of dsRNA treatment were as low as after two days, suggesting that protein depletion is already at a maximum after two days. We observed that many cells did not survive four days of dsRNA treatment and decided to use incubation times of two days for all further experiments. To test the efficiency of proteasome inactivation by simultaneous dsRNA mediated knockdown of Prosalpha5, Prosbeta6 and RPN11 (referred to as "3xKD") treatment, cell lysates were analyzed for the presence of ubiquitinated proteins. The immunostaining patterns are comparable to those observed upon MG132/Lactacystin treatment for 16 h (Figure 1A, B), suggesting that the effect of proteasome activity intervention in terms of accumulation of ubiquitinated proteins and/or induction of protein ubiquitination was similar. dsRNA mediated knockdown, in contrast, results in subunit depletion and may therefore also affect proteasome structure and assembly. Indeed, 3xKD resulted in an at least partial disruption of the proteasome structure as suggested by glycerol density gradient centrifugation assays (Figure S1B). In contrast, MG132/Lactacystin treated proteasome samples showed a pattern that is indicative of intact proteasomes (fractions #7-9), but, in addition, suggested an increased presence of alpha subunits in the lower density fractions. The overall staining intensities increased in both cases, even though the total protein input amounts were kept constant. This suggests an abundance increase

of proteasome constituents as a result of these treatments, which was confirmed by the quantitative proteomics experiments described below while similar effects have been observed by others (Lundgren *et al.*, 2003, 2005; Szlanka *et al.*, 2003). In general, proteins with high turnover rates, such as cyclins, are expected to become deregulated upon proteasome malfunctioning. Cell cycle regulation is a process that particularly relies on the proper regulation of such proteins. We observed a disturbance of the cell cycle upon both perturbations by FACS analysis. The higher G2/M phase peak and the lower G1 phase peak compared to the control situation indicate a G2/M arrest in the affected cells (Figure S1C). One possible explanation is that cells go into apoptosis, which is also suggested by the upregulation of typical apoptosis markers (shown hereafter). In conclusion, both dsRNA mediated knockdown and treatment with chemical inhibitors interfere with proteasome functioning, result in elevated levels of ubiquitinated proteins and affect cell cycle regulation.

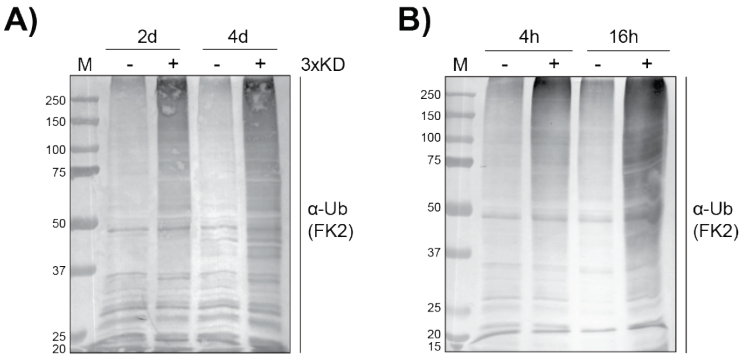

C)

Experiment	Mixing type	Light state	Heavy state
4 h inhibitor	Forward	Treated sample	Control
4 h inhibitor	Reverse	Control	Treated sample
16 h inhibitor	Forward	Treated sample	Control
16 h inhibitor	Reverse	Control	Treated sample
2 d 3x knockdown	Forward	Treated sample	Control
2 d 3x knockdown	Reverse	Control	Treated sample
4 d 3x knockdown	Forward	Treated sample	Control
4 d 3x knockdown	Reverse	Control	Treated sample

Figure 1. Immunoblots of proteasome samples treated with 3xKD (A) or MG132/Lactacystin (B) stained with FK2 antibody that recognizes conjugated ubiquitin branches, showed that global ubiquitination increases as a result of proteasome inactivation. C) Experimental design: SILAC samples were prepared in a forward and reverse manner to generate independent duplicates.

Next, we set out to investigate the effect of proteasome dysfunction on the global cellular proteome using a SILAC based mass spectrometry approach (Figure 1C). All experiments were performed in duplicate in a forward and reverse fashion, meaning that the SILAC labels were swapped for the duplicate experiment to correct for irregularities as a result of the stable isotope labeling procedure. Typically, over 5,000 proteins were identified and quantified per SILAC assay, with a total number of 5,899 proteins over all analyses (Table 1). Proteins with >1.5-fold abundance differences were defined as upregulated/accumulated or downregulated and were only selected for further analysis if consistent ratios in the forward and reverse experiments were observed.

Table 1. Numbers of identified up- and downregulated proteins.

Experiment	Exp #1	Exp #2	Total Exp #1 or Exp #2	Up in Exp #1	Up in Exp #2	Up in Exp #1 and Exp #2	Down in Exp #1	Down in Exp #2	Down in Exp #1 and Exp #2
4 h inhibitors	4862	4801	5056	223	212	78	45	66	1
16 h inhibitors	5025	5035	5282	749	723	466	90	74	11
2 d 3xKD	5166	5225	5367	851	769	545	139	162	50
4 d 3xKD	5128	5068	5331	922	939	598	287	355	109

Upon 16 h treatment with MG132/Lactacystin and upon 3xKD, more than 10% of the total measurable proteome was affected (Table 1, Figure S3). The dynamics of protein abundance and extent of upregulation are visualized in Figure 2 (see Table S1 for a complete list of proteins). After 4 h of treatment with chemical inhibitors a small set of stress responsive proteins were already extensively upregulated. These included the heat shock proteins Hsp22, Hsp23, Hsp26, Hsp70 and Hsp27, which have been shown to physically interact with the proteasome (Parcellier *et al.*, 2003) and to be induced upon proteasome inactivation (Lee and Goldberg, 1998b). Heat shock proteins remained present at highly elevated levels during prolonged exposure to inhibitors, as well as in 3xKD, suggesting that the cell maintains its stress responsive state as long as the proteasome's activity is reduced. Heat shock factor 1 (Hsf1), a master regulator of the heat shock genes that plays a significant role in suppressing protein misfolding in cells by

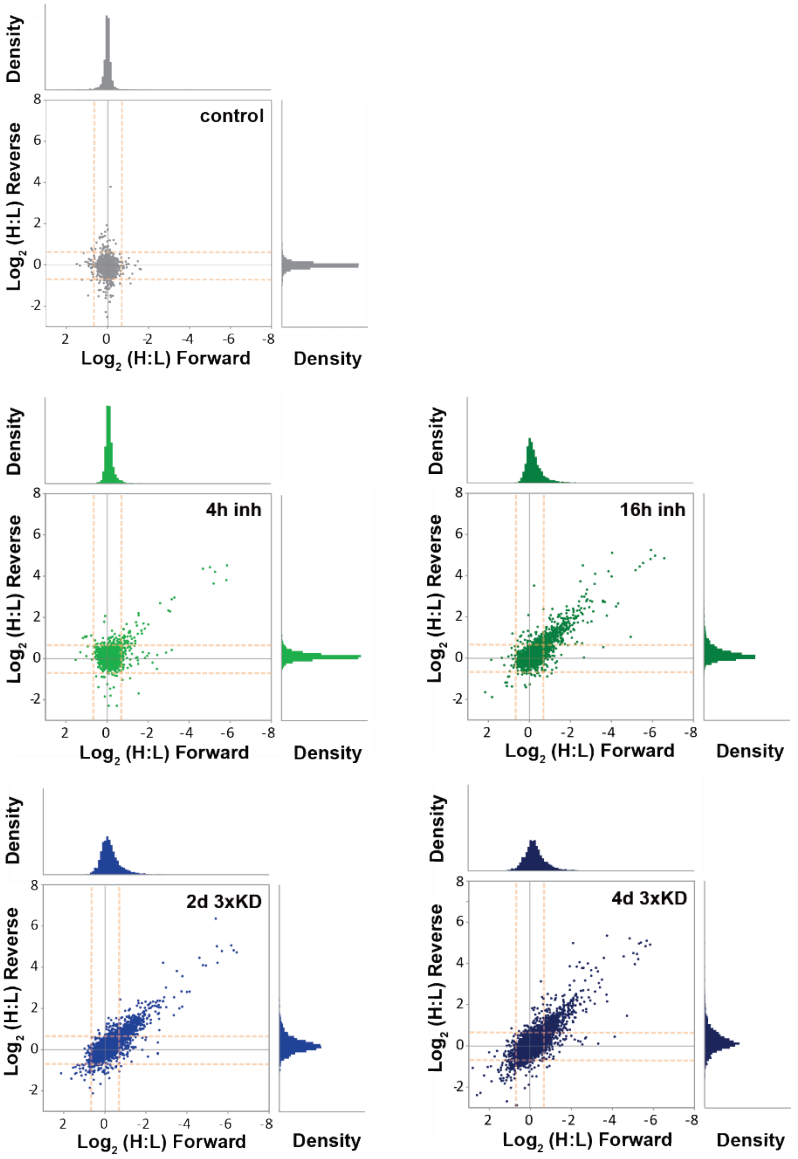

Figure 2. H:L ratios from forward and reverse SILAC experiments for the complete protein population and their distribution around the axis centers showed that a substantial part of the global proteome was remodeled. The H:L threshold ratio of 1.5-fold (corresponding to 0.59 at the Log2 scale) is indicated by the orange dashed line. The distribution of data points becomes less narrow as a result of proteasome perturbation, either with drugs or by dsRNA mediated knockdown of subunits.

inducing the expression of heat shock genes (Schubert *et al.*, 2000), is also present at elevated concentrations under all conditions tested. Ref(2)p, which has a ubiquitin binding domain and has been shown to localize to ubiquitin-positive protein aggregates (Nezis *et al.*, 2008), was increased to a similar extent as the heat shock proteins. Other 'early responders' included Pomp, the *Drosophila* homolog of human Ump1, a short-lived chaperone present in the precursor form of 20S that is required for the correct assembly and enzymatic activation of the proteasome (Ramos *et al.*, 1998; Burri *et al.*, 2000).

In general, the overlap between 16h drug treatment and 3xKD was quite extensive in spite of the slightly different time scales at which the perturbation mechanisms act (Figure 3). Gene Ontology (GO) analysis revealed that shared proteins include stress response proteins and proteins involved in the UPS, apoptosis, transcription and cell signaling (Figure S4). In addition, while upregulated proteins in the chemical inhibition experiments were enriched for in functional categories such as metabolic processes and development, increased proteins in 3xKD were also related to cytoskeleton organization and cell proliferation. Approximately 50 proteins were increased in all conditions, including additional stress response proteins such as DnaJ protein homolog, Methuselah and Thor. Proteins involved in the JNK cascade, Kayak (Fos), Jra (AP-1) and the phosphatase Puckered, as well as the transcription factors Apterous, Helix loop helix protein 106 and the transcriptional repressor Hairy were increased. Upregulated proteins involved in apoptosis included the Bcl-2 family member protein Debcl (dBorg or BG1), a key regulator of apoptosis (Quinn *et al.*, 2003), as well as Dcp-1, Diap (Thread/th), Dredd (Caspase-8), Drice (Caspase), Strica/Dream, UbcD1 (effete/eff) and Morgue. Ago, the substrate recognition component of a SKP1-CUL1-F-box protein E3 ubiquitin-protein ligase complex mediating the ubiquitination and subsequent proteasomal degradation of target proteins, also showed increased abundance in all cases. Cell cycle regulators (CycA, CycB, CycK CycH, CycE and Cks85A), mitotic spindle related proteins and c-Myc (dm) were also affected.

Interestingly, the relatively small pool of downregulated proteins in 3xKD consisted almost exclusively of mitochondrial ribosomal proteins (Figure 3A, Table S1). The perturbation of mitochondria has been described as a cellular event that follows the initial accumulation of short-lived proteins and concomitant induction of apoptosis by proteasome inhibition (Almond and Cohen, 2002). Also, a similar decline of ribosomal proteins and concomitant increase in proteasome complex constituents was recently observed in aging experiments in *C. elegans* (Walther *et al.*, 2015).

The global abundance levels of ubiquitin increased two- to five-fold upon proteasome inactivation (Figure S7). A bottom-up proteomics assay does not allow the differentiation between conjugated, polymeric, monomeric, free and activated ubiquitin and so the detected proteolytic fragments merely reflect all ubiquitin present in the cell. Using 'tryptic' proteomics it is however possible to identify and quantify the various linkage types of polyubiquitin in detail.

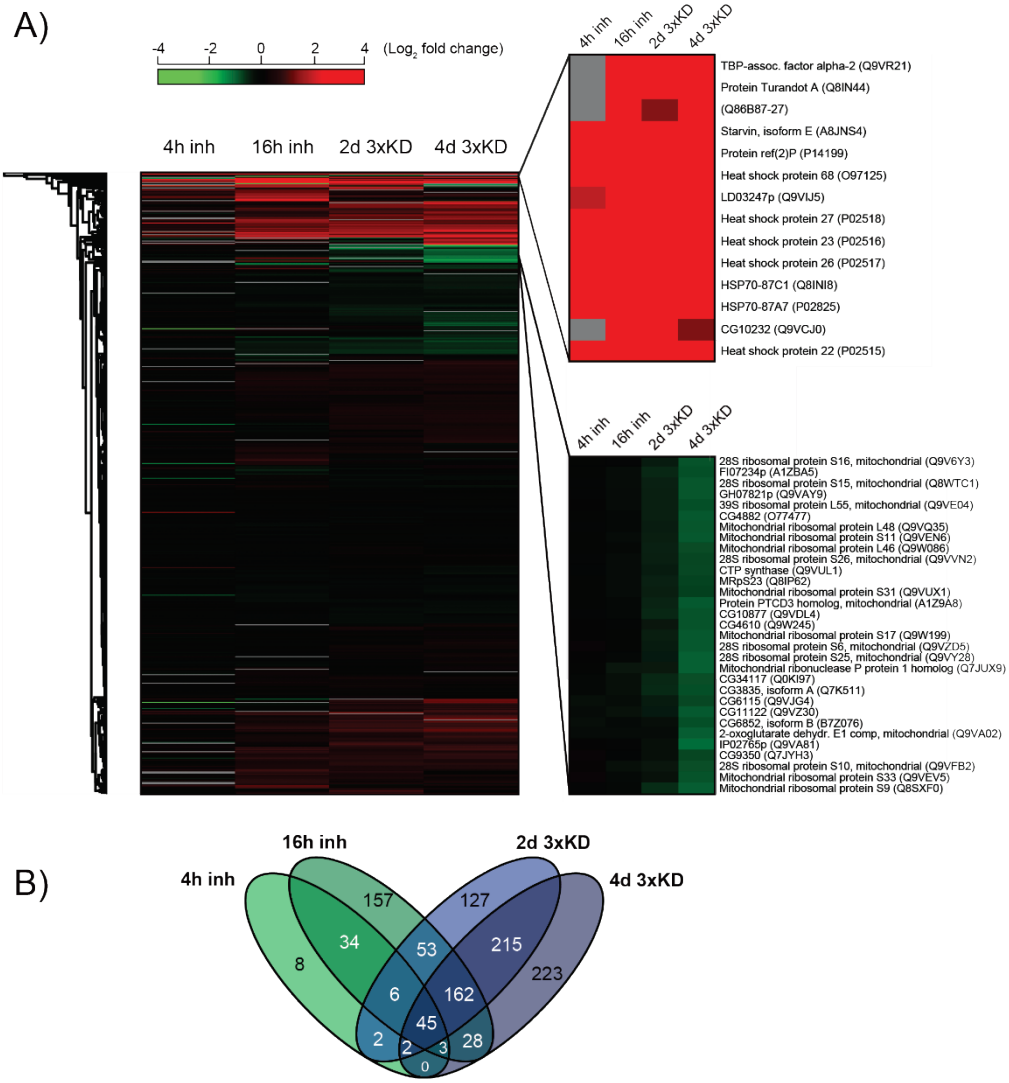

Figure 3. Clustering analysis revealed that many affected proteins in the 3xKD and chemical inhibitors experiments overlap (A, B). The magnification shows a subset of typical proteins that are upregulated in all conditions (red). Notably, many of the proteins that decreased in abundance in 4d 3xKD were related to the mitochondrial ribosome (magnified area, green). A complete list of proteins can be found in Supplementary Table 1.

An extensive analysis of the polyubiquitin dynamics is described in the 'ubiquitinome' section below. In addition, all proteasome subunits, except for Prosbeta7 in 3xKD, were increased upon inactivation by inhibition and subunit knockdown (Figure S7). This phenomenon, also observed by others (Wójcik and DeMartino, 2002; Lundgren *et al.*, 2005), may either be a consequence of the high turnover of proteasome subunits or may be an effect of elevated expression to compensate for loss of proteasomal activity sensed by the cell.

Next, we sought to determine whether the observed increased abundances are the result of protein accumulation or rather of *de novo* protein synthesis. For this, we combined proteasome inhibition with cycloheximide (CHX) treatment, which blocks the translational elongation thus inhibiting protein biosynthesis, in a SILAC based assay. Cells were either treated with CHX and MG132/Lactacystin for 4 hours or with MG132/Lactacystin alone, while CHX was added to the cell culture one hour prior to MG132/Lactacystin. Proteins with abundance dynamics effects upon CHX treatment, but non-responsive upon inhibitor treatment, were excluded from downstream analysis. The majority of proteins were indeed increased as a result of *de novo* synthesis (Figure 4, Table S2). Interestingly, ubiquitin was also *de novo* synthesized. While ubiquitin is recycled by specific proteasome modules and not degraded along with proteasome targeted proteins, the total ubiquitin pool in the cell is expected to be rather stable in proteostasis conditions. We hypothesize that the existing pool of ubiquitin is apparently not sufficient to accommodate for the need of ubiquitin under the here imposed stress conditions. This idea is supported by data from Kopito and coworkers on mouse embryonic fibroblasts (MEFs), who showed that proteasome inhibition leads to a robust increase in total ubiquitin because of transcriptional activation of ubiquitin gene expression, although this effect is cell type dependent (Kaiser *et al.*, 2011).

In conclusion, a substantial part of the proteome that was upregulated after proteasome inactivation consists of *de novo* synthesized proteins. Unfortunately, CHX treatment could not be prolonged for more than 4 hours, because longer incubation turned out to be lethal to S2 cells. It is expected that after prolonged inactivation the accumulation of polyubiquitinated proteins destined for degradation becomes an increasingly important factor to explain observed elevated protein abundances.

In order to understand how proteasome inactivation disturbs UPS regulation, we then focused on the analysis of protein ubiquitination. Since proteins destined for degradation by the proteasome carry a polyubiquitin tag, disruptions of the UPS are expected to result in substantial changes at the ubiquitin-modified proteome ('ubiquitinome') level. Ubiquitinome analysis revealed over 14,000 unique diGly peptides that were identified over all SILAC experiments (Table 2, Table S3), the majority of which could also be quantified.

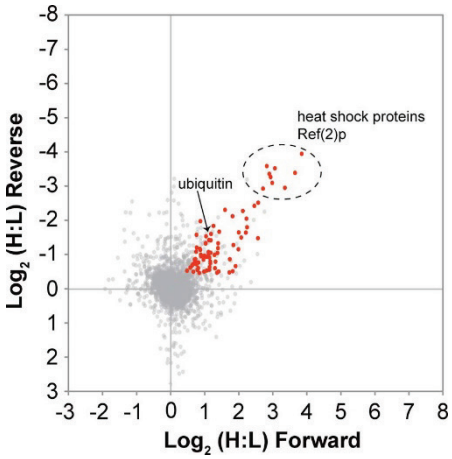

Figure 4. A comparison of cells that were treated with a combination of the translational inhibitor cycloheximide (CHX) and MG132/Lactacystin, and control cells treated with MG132/Lactacystin alone, revealed that the majority of the increased proteins upon proteasome inhibition were indeed synthesized but not accumulated. Red data points represent proteins that were also present with increased abundances in the MG132/Lactacystin *vs* untreated cells screen. For a complete list of synthesized proteins, see Supplementary Table 2.

Since, to our knowledge, this is the first large-scale ubiquitinome screen in *Drosophila*, we set out by searching for potential ubiquitination target consensus sites. A sequence context (motif) analysis carried out to determine how Lys ubiquitination may be regulated at the primary structure level did not reveal any consensus ubiquitination site whatsoever (Figure S5A). This is in agreement with a study in mammalian cells in which no enrichment for any particular motif was observed either (Kim, Eric J. Bennett, *et al.*, 2011). While for non-modified peptides there was a clear correlation between the number of identified peptides per protein corrected for the corresponding protein molecular mass on the one hand and the total protein intensity on the other hand, no such correlation was observed for diGly peptides (Figure S5B). This indicates that diGly peptides were not detected because they originate from abundant proteins *per se*. Instead, it suggests that the extent of ubiquitination is highly variable per protein and independent of absolute protein abundance levels. The overlap of diGly peptides that were identified in the various data sets was reasonable, but not extensive (Figure S5C). There may be both experimental and biological explanations for this. Different strategies to inactivate the proteasome may result in partially different ubiquitinome transformation effects, or degradation directed protein ubiquitination may not occur in a site-specific fashion. Also, we cannot exclude the possibility that only a fraction of the total ubiquitinome is captured in these diGly IP's. After 4 h proteasome inhibition ubiquitinome transformation may still be in its infancy and many of the target sites may not yet be modified, or their stoichiometry is too low so that they will simply

escape detection. The absolute intensities of diGly peptides of ubiquitin were roughly two orders of magnitude lower than those for its non-modified peptides (Figure S5D), which indeed indicates a low stoichiometry of ubiquitination modification.

Table 2. Numbers of identified and quantified diGly peptides over all experiments.

	# of diGly peptides
Total identified (heavy or light)	22,614
Total identified (heavy and light counterparts collapsed)	14,018
with 1 diGly site	13,641
with 2 diGly sites	344
with 3 diGly sites	28
with 4 diGly sites	5
Total identified and quantified	11,091
no reported H:L ratio in forward and reverse experiment	1,268
intensity value reported in only light channel or heavy channel	1,097

Next, we interrogated the dynamics of protein ubiquitination as a result of proteasome inactivation in a diGly peptide SILAC assay. Over 70% of all identified diGly peptides showed increased abundances as a result of proteasome inactivation (Figure 5A). For ubiquitination sites detected in multiple perturbation types, there was a substantial overlap in upregulation (Figure 5B). Proteins with increased ubiquitin modification were involved in diverse processes such as cell cycle regulation, (ubiquitin-dependent) protein catabolism, cytoskeleton and mitotic spindle organization, apoptosis, proteolysis and metabolism and have ubiquitin ligase, nucleotide binding and ATPase activities (Figure S6). There were no obvious differences in GO enrichment profiles between the different treatments.

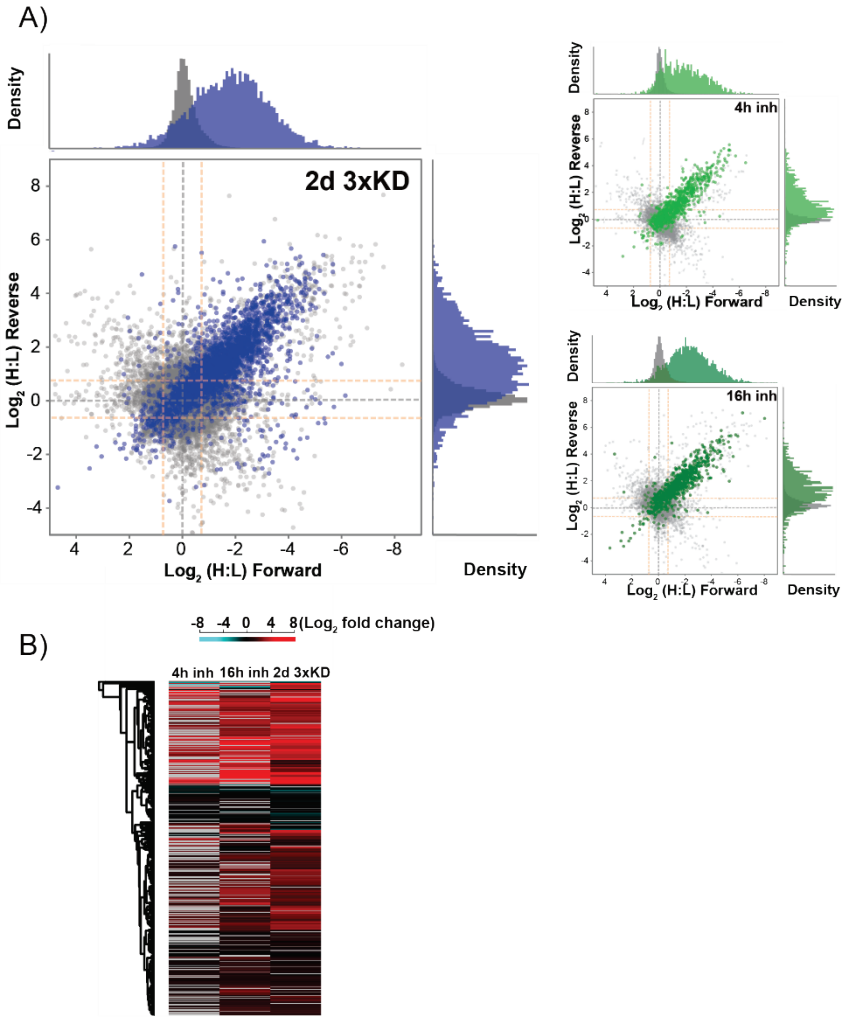

Figure 5. A) H:L ratios of non-modified (grey) and diGly (blue) peptides from the 2d 3xKD proteasome inactivation duplicate experiment. The deviation of the virtually complete diGly peptide population from the axis center indicates an enormous remodeling of the total ubiquitinome, while the remodeling of the non-modified peptidome was relatively limited (see also Figure 2 for global proteome profiles). B) Clustering analysis of diGly peptide dynamics revealed that there is a substantial overlap between the inhibition and knockdown experiments. Obviously, after relatively short incubation times, many of the diGly peptides were not upregulated yet.

We then integrated the protein abundance dynamics data with the associated dynamic ubiquitination profiles, which resulted in the formation of different categories of proteins with specific associations of ubiquitination profile and abundance dynamics (Figure 6, Table S4). Representative examples of each of these categories are discussed in more detail. The first - and largest - category consisted of proteins combining overall increased ubiquitination at all identified target sites with increased global abundance As an example Proasalpha1 is shown, although all proteasome subunits display a similar behavior. Proteins with abundance changes accompanied by larger fold changes of diGly peptides are exemplified by Q7KN62. A third class is represented by Sgt, whose global abundance remained largely unchanged, although its site ubiquitination occupancy increased several fold. Besides these major categories, proteins were identified with opposite ubiquitination and abundance regulation behavior. One example is sta: while the overall protein abundance decreased, ubiquitination occupancies at several target sites increased.

For several other proteins different ubiquitination sites were identified with opposite dynamic behavior. For instance, CG5174 displayed a relatively stable global abundance level, but simultaneous heterogeneous ubiquitination. Similarly, the overall level of BTF3 remained constant, whereas at least one diGly peptide decreased three-fold. While the decrease of global RpL5 and RpS10b levels may be a result of decreased biosynthesis rates, it is more difficult to explain their dynamic ubiquitination profile. For RpL5, most ubiquitination sites were upregulated, but one site was downregulated. In contrast, for RpS10b most, but not all, ubiquitination sites were downregulated.

An intriguing example is RpS3, a constituent of the ribosome that is known to also have extra-ribosomal roles such as involvement in the repair of UV-induced DNA damage (Wilson 3rd, Deutsch and Kelley, 1993) and as an inducer of apoptosis (Jang, Lee and Kim, 2004). Its overall abundance decreased slightly, while the diGly peptide dynamics displayed an extremely heterogeneous profile. Remarkably, all downregulated ubiquitination sites are exclusively localized in the unstructured C-terminal domain, while all upregulated target sites are restricted to the structured domain (Figure 6B). One possibility is that the reported diGly peptides originate from different populations of RpS3, *e.g.* in isolated subcellular compartments. Alternatively, if the identified ubiquitination sites indeed coexist on the same individual RpS3 molecule and represent degradation signals, it would suggest opposing degradation signaling dynamics in different protein domains. Interestingly, it was shown recently that the proteasome prefers substrates that have disordered regions with complex amino acid composition to initiate degradation (Fishbain *et al.*, 2015; Humbard and Maurizi, 2015). Another possibility is that the structured and unstructured domains may be physically separated entities. Partial proteasomal degradation, ranging from complete degradation to complete protection of one particular domain, has been observed in *e.g.* signaling pathways (Kraut and Matouschek, 2011). However, perhaps the most likely explanation is that, while some of the ubiquitination sites may represent proteasomal degradation marks, others are involved in regulatory events.

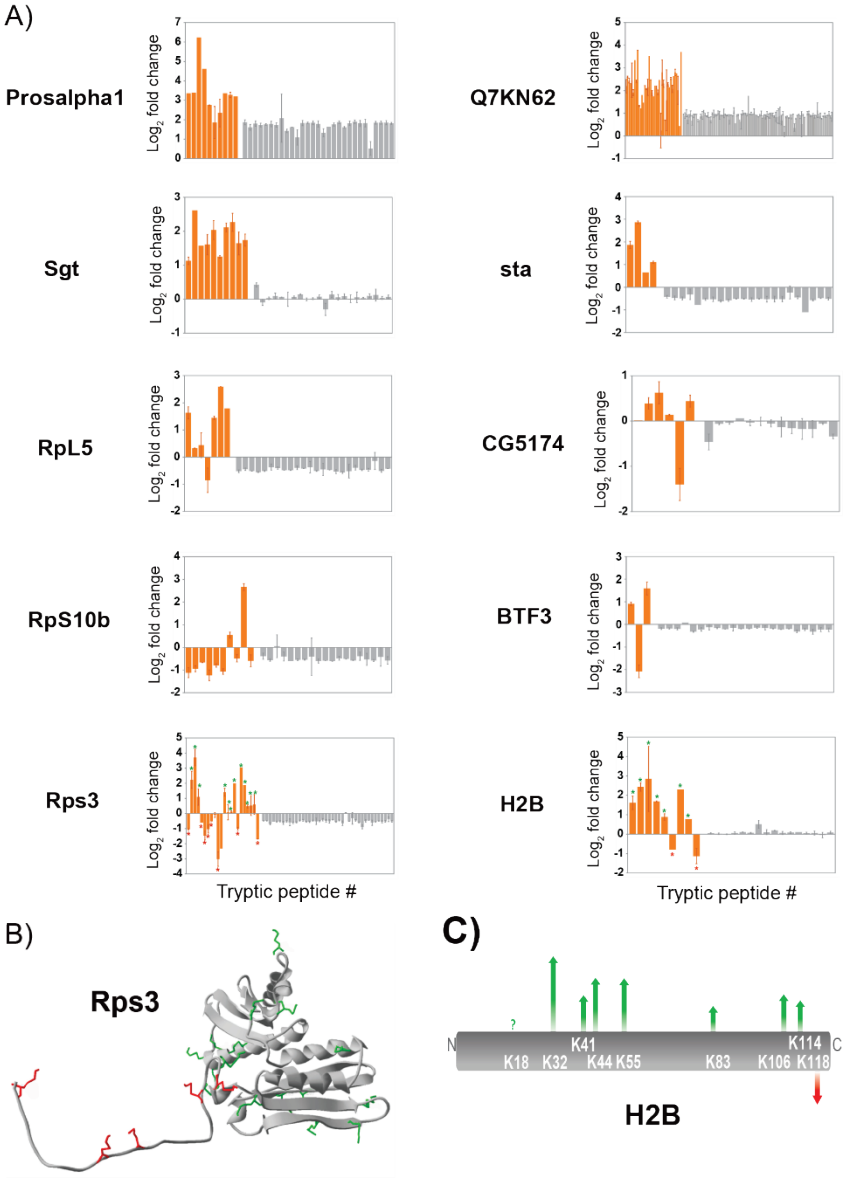

Figure 6. A) Dynamics of diGly (orange) and non-modified (grey) peptides upon proteasome inactivation for a selection of proteins. Fold change values are an average of at least two independent measurements, unless no error bar is indicated; the ranking of peptides on the x-axis is at random and does not reflect the position in the protein sequence. Multiple different diGly peptides may contain the same modified Lys residue. A question mark indicates that although diGly site was identified, the quantitative information data

quality was insufficient. B) Three–dimensional structure of the *Drosophila melanogaster* 40S ribosomal protein S3 based on PDB accession 4v6w (RpS3 / CG6779; chain AD; protein length 246) (Anger *et al.*, 2013). Lys residues with decreasing ubiquitination are indicated in red, Lys residues with increasing ubiquitination in green; the same color coding applies to Rps3 in Panel A. Two additional C-terminal Lys residues that were quantified with decreasing ubiquitination in the SILAC assay were not present in the 3D-structure (*i.e.*, K235 and K244). C) Schematic representation of the primary structure of histone H2B. The Lys residues that showed increased (green) or decreased (red) ubiquitination are indicated; color coding corresponds to the bar graph for H2B in Panel A. Multiple diGly peptides may represent the same ubiquitination site.

This hypothesis is supported by recent work from Higgins *et al.* (Higgins *et al.*, 2015), who identified similar RpS3 ubiquitination patterns suggesting that a subset of 40S ubiquitylation events must be regulatory in nature. This idea is consolidated by reports that ~65% of ubiquitin is present as monoubiquitinated substrates in mammalian cell lines (Kaiser *et al.*, 2011) and, thus, has regulatory functions. Another interesting case was presented by histone H2B (Figure 6C). All ubiquitination sites were upregulated, except for K118. It is known that monoubiquitination of this particular residue is a regulatory modification that plays a key role in transcriptional activation (Zhang, 2003), while other ubiquitination sites in (human) H2B have been identified although these are not well studied or understood yet (Molden *et al.*, 2015). One possibility is that the observed decreased ubiquitination at K118 indeed represents monoubiquitination and is the result of the stress imposed by proteasome inactivation that leads to a global decrease of transcription and protein synthesis such as has been observed for example in the case of ER stress that activates the unfolded protein response (Walter and Ron, 2011).

Our findings are in partial contrast to those of Kim *et al.* (Kim, Eric J. Bennett, *et al.*, 2011), who observed a similar decrease of diGly peptide representing this particular Lys (corresponding to K121 in human H2B), but a decrease instead of an increase of two other diGly sites. It should be noted that the coverage of diGly sites in our screen is higher (7 versus 3), that the timescale between chemical and dsRNA mediated proteasome inactivation may be different and that other cell types were used. In conclusion, the heterogeneous ubiquitination dynamics within proteins forms an intriguing observation. Further investigation should be focused on the identification of the linkage type of the (poly)ubiquitin modifications to differentiate between degradation marks and regulatory ubiquitination.

The analysis of diGly peptides from polyubiquitin allowed us to investigate whether there is a preference for specific linkage types at a global scale under the conditions tested. All chain types increased in all conditions, with no clear preference for K48-linked chains or any other chain type (Figure 7, Table S5). Surprisingly, only K27-linked chains stand out in the 16h MG132/Lactacystin and 3xKD experiments and show a slightly higher fold upregulation than the other linkage types. K27-linked polyubiquitin was recently shown to be required for promoting chromatin ubiquitination following DNA damage, which seemed strictly dependent on the activity of the ubiquitin ligase RNF168 (Gatti *et al.*, 2015). Whether or not K27-linked

polyubiquitin indeed plays a special role here needs to be investigated further. Although K48-linked polyubiquitin chains are widely held to be the canonical signal for proteasome-mediated degradation, other polyubiquitin linkage types have also been implicated in proteasomal targeting. For instance, Kaiser *et al.* observed a two-fold increase in all polyubiquitin linkages in HEK293 cells after treatment with MG132, while in MEF cells a ten-fold increase in K48-linked chains and a three- to four-fold increase in K63- and K11-linked chains was measured (Kaiser *et al.*, 2011). In another report, Meierhofer *et al.* (Meierhofer *et al.*, 2008) observed no clear chain linkage preference in HeLa cells and even measure slightly higher fold increases for K6-, K11-, K27- and K33-linked chains than for K48-linked chains upon proteasome inactivation. The accumulation of other chains than K48-linked suggests that cells could use multiple types of polyubiquitin chains as proteasome-targeting signals or may reflect the existence of mixed-linkage polyubiquitin chains or of multiple chain types on individual proteins. Alternatively, secondary effects involving other types of polyubiquitin signaling may accompany proteasome mediated degradation. Overall, the abundance increases were slightly higher for the diGly peptides than for the non-modified peptides of ubiquitin, indicating that a relatively larger fraction of ubiquitin resided in polyubiquitin structures upon proteasome perturbation and may suggest that ubiquitin is recruited for the formation of ubiquitin polymers from other pools.

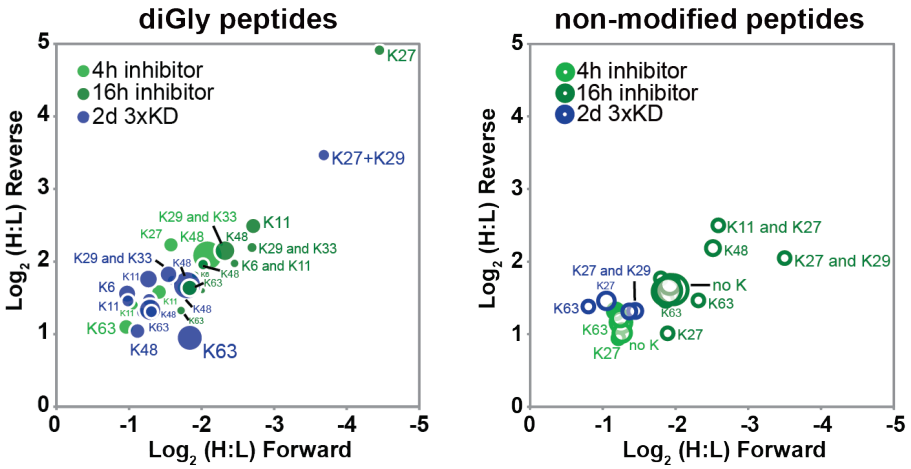

Figure 7. Polyubiquitin linkage types: ubiquitin diGly peptides (closed circles, left panel) contain the indicated Lys as the modified and (as a result of missed cleavage) non-C-terminal residue. The increase of ubiquitin diGly peptides under proteasome inactivation conditions did not show a clear bias towards the canonical proteasomal degradation K48-linkage type. The non-modified tryptic peptides (open circles, right panel) contain the indicated Lys residues in most cases as the C-terminal residue. Tryptic ubiquitin peptides without any Lys residue are indicated by 'no K'. In several cases, multiple peptides representing the same linkage type were identified. The size of the bullets represents the relative peptide count. Smaller circles represent relatively low abundant peptides and may therefore have larger quantitation errors.

Conclusions

We have shown here that the global proteome and, to a greater extent, the ubiquitinome are severely modified upon proteasome inactivation both by chemical inhibitors and by dsRNA mediated knockdown of specific subunits in *Drosophila* S2 cells. Affected ubiquitin-mediated protein degradation by decreased proteasome activity would lead to accumulation of polyubiquitin modified proteins. Therefore, the extent of protein accumulation would develop in parallel to the increase of ubiquitination stoichiometry. Based on mass spectral intensity analysis we have shown that the absolute ubiquitination stoichiometries are relatively low, which is in agreement with earlier observations of Kim *et al.* (Kim, Eric J. Bennett, *et al.*, 2011). Many proteins exhibit irregular ubiquitination profiles, with simultaneous increasing and decreasing site-specific ubiquitination within the same protein, with no apparent relationship to their overall protein abundance levels. Most likely, part of these ubiquitination events has non-degradative regulatory functions.

In our assay, 3,077 proteins with at least one diGly peptide were identified. With 5,899 proteins identified in total, this means that at least 52% of all proteins carry a ubiquitin modification, at least under proteotoxic conditions. We argue that proteins that do not represent conventional proteasome substrates, such as proteins that are part of ubiquitin signaling networks and that carry regulatory (poly)ubiquitin marks different from the canonical K48-linked polyubiquitin degradation signal mark, may represent a wide cross-section of the diGly-containing proteome, which has also been suggested by others (Kim, Eric J. Bennett, *et al.*, 2011; Komander and Rape, 2012). The fact that ~65% of ubiquitin is present as monoubiquitinated substrates in mammalian cell lines, as was reported by Kaiser *et al.* (Kaiser *et al.*, 2011), supports this hypothesis. As a result of tryptic cleavage in bottom-up proteomics approaches, it is not possible to differentiate between mono-, di- and polyubiquitination using the diGly enrichment protocol described here. It would be extremely interesting to be able to differentiate between structurally different ubiquitination modifications in this high-throughput assay, since this would shed more light on the various cellular functions and the relationship between these functions and the exact structure of polyubiquitin moieties.

In conclusion, we have shown that combining quantitative proteomics with dsRNA mediated knockdown of individual subunits of the 26S proteasome complex in *Drosophila* offers a powerful and easy to implement tool to study the dynamics of the (modified) proteome upon perturbation of the UPS. This strategy may pave the path for the dissection of the mode of action of this intriguing cellular machinery by screening individual subunit knocking downs in a systematic way, both under proteostasis as well as proteotoxic conditions. For instance, it is unclear why the 26S proteasome contains three different DUBs and the details of the interplay between them and the ubiquitin receptor proteins are not known. Targeted depletion of each of these proteins could present a far more subtle interference with proteasome functioning than using possibly

unspecific chemical inhibitors. Understanding the details of proteasome functioning is essential for the development of next generation proteasome inhibitors for clinical purposes. Finally, since this is to our knowledge the first comprehensive ubiquitinome screen in a fruit fly cell system, so this data set will serve as a valuable repository for the *Drosophila* community at large.

Supporting information available online

TABLE S1 - List of identified and quantified proteins in the global proteome assay.

TABLE S2 - List of *de novo* synthesized proteins.

TABLE S3 - List of identified and quantified diGly peptides.

TABLE S4 - List of all quantified non-modified and diGly peptides.

TABLE S5 - List of all quantified peptides of ubiquitin.

FIGURE S1 – Proteasome integrity and cell cycle regulation upon inhibition and 3xKD.

FIGURE S2 – Volcano plots showing significantly up- and downregulated proteins upon inhibition and 3xKD.

FIGURE S3 - Percentages of up- and downregulated proteins upon inhibition and 3xKD.

FIGURE S4 - Gene Ontology (GO) analysis of affected proteins upon inhibition and 3xKD.

FIGURE S5 - Consensus site analysis, mass spectral intensities and overlap of identified diGly peptides.

FIGURE S6 - GO analysis of upregulated diGly peptides upon inhibition and 3xKD.

FIGURE S7 - Upregulation of ubiquitin and proteasome subunits upon proteasome inactivation.

References

Almond, J. B. and Cohen, G. M. (2002) 'The proteasome: a novel target for cancer chemotherapy', *Leukemia*. 2002/04/18, 16(4), pp. 433–443.

Anger, A. M. *et al.* (2013) 'Structures of the human and Drosophila 80S ribosome', *Nature*. 2013/05/03, 497(7447), pp. 80–85.

Brand, A. H. and Perrimon, N. (1993) 'Targeted gene expression as a means of altering cell fates and generating dominant phenotypes', *Development*, 118(2).

Burri, L. *et al.* (2000) 'Identification and characterization of a mammalian protein interacting with 20S proteasome precursors', *Proc Natl Acad Sci U S A*. 2000/09/06, 97(19), pp. 10348–10353.

Chalkley, G. E. and Verrijzer, C. P. (2004) 'Immuno-Depletion and Purification Strategies to Study Chromatin-Remodeling Factors In Vitro', *Methods in Enzymology*, 377(2001), pp. 421–442.

Chau, V. *et al.* (1989) 'A multiubiquitin chain is confined to specific lysine in a targeted short-lived protein', *Science*. 1989/03/24, 243(4898), pp. 1576–1583.

Chen, Z. J. and Sun, L. J. (2009) 'Nonproteolytic functions of ubiquitin in cell signaling', *Mol Cell*. 2009/02/17, 33(3), pp. 275–286.

Ciechanover, A. and Brundin, P. (2003) 'Review The Ubiquitin Proteasome System in Neurodegenerative Diseases: Sometimes the Chicken, Sometimes the Egg', *Neuron*, 40, pp. 427–446.

Dietzl, G. *et al.* (2007) 'A genome-wide transgenic RNAi library for conditional gene inactivation in Drosophila', *Nature*, 448(7150).

Elena Koulich, Xiaohua Li, and G. N. D. (2008) 'Relative Structural and Functional Roles of Multiple Deubiquitylating Proteins Associated with Mammalian 26S Proteasome', *Molecular biology of the cell*, 19, pp. 1072–1082.

Fenteany, G. *et al.* (1995) 'Inhibition of proteasome activities and subunit-specific amino-terminal threonine modification by lactacystin', *Science*, 268(5211), pp. 726–731.

Fishbain, S. *et al.* (2015) 'Sequence composition of disordered regions fine-tunes protein half-life', *Nat Struct Mol Biol*. 2015/02/03, 22(3), pp. 214–221.

Gatti, M. *et al.* (2015) 'RNF168 promotes noncanonical K27 ubiquitination to signal DNA damage', *Cell Rep*. 2015/01/13, 10(2), pp. 226–238.

Giasson, B. I. and Lee, V. M. (2003) 'Are ubiquitination pathways central to Parkinson's disease?', *Cell*. 2003/07/16, 114(1), pp. 1–8.

Groll, M. *et al.* (2006) 'Crystal structure of the boronic acid-based proteasome inhibitor bortezomib in complex with the yeast 20S proteasome.', *Structure (London, England : 1993)*, 14(3), pp. 451–6.

Hershko, A. and Ciechanover, A. (1998) 'The ubiquitin system.', *Annual review of biochemistry*, 67, pp. 425–79.

Higgins, R. *et al.* (2015) 'The Unfolded Protein Response Triggers Site-Specific Regulatory Ubiquitylation of 40S Ribosomal Proteins', *Molecular Cell*, pp. 1–15.

Huang, D. W. *et al.* (2007) 'DAVID Bioinformatics Resources: expanded annotation database and novel algorithms to better extract biology from large gene lists', *Nucleic Acids Res*. 2007/06/20, 35(suppl_2), pp. W169-75.

Humbard, M. A. and Maurizi, M. R. (2015) 'The proteasome gets a grip on protein complexity', *Nat Struct Mol Biol*. 2015/03/05, 22(3), pp. 181–183.

Iwai, K. and Tokunaga, F. (2009) 'Linear polyubiquitination: a new regulator of NF-kappaB activation', *EMBO Rep*. 2009/06/23, 10(7), pp. 706–713.

Jang, C.-Y., Lee, J. Y. and Kim, J. (2004) 'RpS3, a DNA repair endonuclease and ribosomal protein, is involved in apoptosis', *FEBS Letters*, 560(1–3), pp. 81–85.

Kaiser, S. E. *et al.* (2011) 'Protein standard absolute quantification (PSAQ) method for the measurement of cellular ubiquitin pools.', *Nature methods*, 8(8), pp. 691–6.

Kal, A. J. *et al.* (2000) 'The Drosophila brahma complex is an essential coactivator for the trithorax group protein zeste', *Genes Dev.* 2000/05/16, 14(9), pp. 1058–1071.

Keller, J. N., Gee, J. and Ding, Q. (2002) 'The proteasome in brain aging', *Ageing Res. Rev.* 2002/06/01, 1(2), pp. 279–293.

Kim, W., Bennett, E. J., *et al.* (2011) 'Systematic and quantitative assessment of the ubiquitin modified proteome', *Molecular Cell*, 44(2), pp. 325–340.

Komander, D. (2009) 'The emerging complexity of protein ubiquitination', *Biochem Soc Trans.* 2009/09/17, 37(5), pp. 937–953.

Komander, D. and Rape, M. (2012) 'The Ubiquitin Code', *Annual Review of Biochemistry*, 81(1), pp. 203–229.

Kraut, D. A. and Matouschek, A. (2011) 'Proteasomal degradation from internal sites favors partial proteolysis via remote domain stabilization', *ACS Chem Biol.* 2011/08/06, 6(10), pp. 1087–1095.

Lee, D. H. and Goldberg, A. L. (1998a) 'Proteasome inhibitors: valuable new tools for cell biologists', *Trends Cell Biol.* 1998/10/28, 8(10), pp. 397–403.

Lee, D. H. and Goldberg, A. L. (1998b) 'Proteasome inhibitors cause induction of heat shock proteins and trehalose, which together confer thermotolerance in Saccharomyces cerevisiae', *Mol Cell Biol.* 1998/01/07, 18(1), pp. 30–38.

Li, J. *et al.* (2017) 'Capzimin is a potent and specific inhibitor of proteasome isopeptidase Rpn11', *Nature Chemical Biology*, 13(5), pp. 486–493.

Lundgren, J. *et al.* (2003) 'Use of RNA Interference and Complementation To Study the Function of the Drosophila and Human 26S Proteasome Subunit S13', *Mol Cell Biol*, 23(15), pp. 5320–5330.

Lundgren, J. *et al.* (2005) 'Identification and Characterization of a Drosophila Proteasome Regulatory Network', *Mol Cell Biol.*

Mayor, T. *et al.* (2007) 'Quantitative profiling of ubiquitylated proteins reveals proteasome substrates and the substrate repertoire influenced by the Rpn10 receptor pathway', *Mol Cell Proteomics*. 2007/07/24, 6(11), pp. 1885–1895.

Meierhofer, D. *et al.* (2008) 'Quantitative analysis of global ubiquitination in HeLa cells by mass spectrometry', *J Proteome Res.* 2008/09/11, 7(10), pp. 4566–4576.

Mohrmann, L. *et al.* (2004) 'Differential Targeting of Two Distinct SWI / SNF-Related Drosophila Chromatin-Remodeling Complexes Differential Targeting of Two Distinct SWI / SNF-Related Drosophila Chromatin-Remodeling Complexes', 24(8), pp. 3077–3088.

Molden, R. C. *et al.* (2015) 'Multi-faceted quantitative proteomics analysis of histone H2B isoforms and their modifications', *Epigenetics & Chromatin*. 8(1), p. 15.

Moshkin, Y. M. *et al.* (2007) 'Functional differentiation of SWI/SNF remodelers in transcription and cell cycle control.', *Molecular and cellular biology*, 27, pp. 651–661.

Nezis, I. P. *et al.* (2008) 'Ref(2)P, the Drosophila melanogaster homologue of mammalian p62, is required for the formation of protein aggregates in adult brain', *J Cell Biol.* 2008/03/19, 180(6), pp. 1065–1071.

Ordureau, A., M??nch, C. and Harper, J. W. (2015) 'Quantifying Ubiquitin Signaling', *Molecular Cell*, 58(4), pp. 660–676.

Parcellier, A. *et al.* (2003) 'HSP27 is a ubiquitin-binding protein involved in I-kappaBalpha proteasomal degradation.', *Molecular and cellular biology*, 23(16), pp. 5790–5802.

Ramos, P. C. *et al.* (1998) 'Ump1p is required for proper maturation of the 20S proteasome and becomes its substrate upon completion of the assembly', *Cell*. 1998/03/10, 92(4), pp. 489–499.

Reddy, B. A. *et al.* (2014) 'Nucleotide Biosynthetic Enzyme GMP Synthase Is a TRIM21-Controlled Relay of p53 Stabilization', *Molecular Cell*, 53, pp. 458–470.

San Miguel, J. F. *et al.* (2008) 'Bortezomib plus melphalan and prednisone for initial treatment of multiple myeloma', *N Engl J Med*. 2008/08/30, 359(9), pp. 906–917.

Sap, K. A. *et al.* (2015) 'Global quantitative proteomics reveals novel factors in the ecdysone signaling pathway in Drosophila melanogaster', *Proteomics*, 15(4), pp. 725–738.

Sarraf, S. a. *et al.* (2013) 'Landscape of the PARKIN-dependent ubiquitylome in response to mitochondrial depolarization', *Nature*. Nature Publishing Group, pp. 1–7.

Schubert, U. *et al.* (2000) 'Rapid degradation of a large fraction of newly synthesized proteins by proteasomes', *Nature*. 2000/04/28, 404(6779), pp. 770–774.

Szlanka, T. *et al.* (2003) 'Deletion of proteasomal subunit S5a/Rpn10/p54 causes lethality, multiple mitotic defects and overexpression of proteasomal genes in Drosophila melanogaster', *Journal of Cell Science*, 116(6), pp. 1023–1033.

Thompson, J. W. *et al.* (2014) 'Quantitative Lys-ε-Gly-Gly (diGly) proteomics coupled with inducible RNAi reveals ubiquitin-mediated proteolysis of DNA damage-inducible transcript 4 (DDIT4) by the E3 Ligase HUWE1', *Journal of Biological Chemistry*, 289(42), pp. 28942–28955.

Tyanova, S. *et al.* (2016) 'The Perseus computational platform for comprehensive analysis of (prote)omics data.', *Nature methods*, 13(9), pp. 731–40.

Tyanova, S., Temu, T. and Cox, J. (2016) 'The MaxQuant computational platform for mass spectrometry – based shotgun proteomics', *Nature Protocols*. Nature Publishing Group, 11(12), pp. 2301–2319.

Udeshi, N. D. *et al.* (2013) 'Large-scale identification of ubiquitination sites by mass spectrometry.', *Nature protocols*. Nature Publishing Group, 8(10), pp. 1950–60.

Wagner, S. a *et al.* (2011) 'A Proteome-wide, Quantitative Survey of In Vivo Ubiquitylation Sites Reveals Widespread Regulatory Roles.', *Molecular & cellular proteomics : MCP*, 10(10), p. M111.013284.

Walter, P. and Ron, D. (2011) 'The unfolded protein response: from stress pathway to homeostatic regulation', *Science*. 2011/11/26, 334(6059), pp. 1081–1086.

Walther, D. M. *et al.* (2015) 'Widespread Proteome Remodeling and Aggregation in Aging C. elegans', *Cell*. 2015/05/11, 161(4), pp. 919–932.

Wilson 3rd, D. M., Deutsch, W. A. and Kelley, M. R. (1993) 'Cloning of the Drosophila ribosomal protein S3: another multifunctional ribosomal protein with AP endonuclease DNA repair activity', *Nucleic Acids Res*. 1993/05/25, 21(10), p. 2516.

Wójcik, C. and DeMartino, G. N. (2002) 'Analysis of Drosophila 26 S proteasome using RNA interference.', *The Journal of biological chemistry*, 277(8), pp. 6188–97.

Worby, C. A., Simonson-Leff, N. and Dixon, J. E. (2001) 'RNA interference of gene expression (RNAi) in cultured Drosophila cells.', *Science's STKE : signal transduction knowledge environment*. United States, 2001(95), p. pl1.

Xu, P. *et al.* (2009) 'Quantitative Proteomics Reveals the Function of Unconventional Ubiquitin Chains in Proteasomal Degradation', *Cell*, 137(1), pp. 133–145.

Yeh, C. H., Jansen, M. and Schmidt-Glenewinkel, T. (2011) 'Role of the proteasome in fly models of neurodegeneration', *Methods Mol Biol*. 2011/09/14, 793, pp. 149–165.

Zhang, Y. (2003) 'Transcriptional regulation by histone ubiquitination and deubiquitination', *Genes Dev*. 2003/11/25, 17(22), pp. 2733–2740.